Biochimica et Biophysica Acta, 727 (1983) 22–30
Elsevier Biomedical Press

BBA 71493

EFFECT OF THE LIPID PHASE TRANSITION ON THE KINETICS OF H^+/OH^- DIFFUSION ACROSS PHOSPHATIDIC ACID BILAYERS

KHALID ELAMRANI and ALFRED BLUME

Institut fuer physikalische Chemie II, Albertstrasse 23a, D-7800 Freiburg (F.R.G.)

(Received July 1st, 1982)

Key words: H^+/OH^- diffusion; Phosphatidic acid; Vesicle; Phase transition

The kinetics of H^+/OH^- diffusion across dimyristoyl phosphatidic acid bilayer membranes was measured by following the absorbance of the pH-sensitive indicator Cresol red (*o*-cresolsulfonphthalein) entrapped in single lamellar vesicles after rapidly changing the external pH in a stopped-flow apparatus. The H^+/OH^--permeability coefficient was found to be in the 10^{-5} to 10^{-3} cm·s^{-1} range. The lipid phase transition has a strong influence on the permeation kinetics as the permeability coefficients in the liquid-crystalline phase are drastically higher. The permeability shows no maximum at the phase transition temperature as is the case for other ions, but displays a similar temperature dependence as water permeation. This is also reflected in the high activation energy of approx. 20 kcal/mol and supports the hypothesis (Nichols, J.W. and Deamer, D.W. (1980) Proc. Natl. Acad. Sci. U.S.A. 77, 2038–2042) of H^+/OH^- permeation via hydrogen bonded water molecules. A second slower kinetic phase is also observed, where the permeation is obviously controlled by counterion diffusion. The temperature dependence of this slow process displays the for ion diffusion characteristic maximum in the permeability at the phase-transition temperature.

Introduction

Numerous important membrane-related processes like active transport, oxidative phosphorylation in mitochondria or photophosphorylation in chloroplasts are coupled to an electrochemical gradient of H^+ or OH^- across the membrane. The elucidation of the passive permeation kinetics of these ions is therefore of great interest [1–4]. However, the investigation of the H^+/OH^--permeability of lipid bilayers as model systems for biological membranes has led to large discrepancies in the measured permeability coefficients. Values between 10^{-11} and 10^{-4} cm·s^{-1} have been reported [5–12]. In the course of our studies on the pH-induced phase-transition kinetics of phosphatidic acid bilayers (Elamrani, K. and Blume, A., to be published) it became necessary to measure the H^+/OH^--permability of dimyristoyl phosphatidic acid (DMPA) bilayers and determine the influence of the gel to liquid crystalline phase transition on this process. Several investigations of the permeability properties of lipid model systems have shown that at the phase transition a characteristic increase in the permability coefficient for ions or large hydrophilic molecules is observed whereas the permability of water shows only a sudden increase [13–20]. An analysis of the temperature dependence of the H^+/OH^--permeability coefficient across the phase-transition region could therefore give new insight into the mechanism of H^+/OH^--permeation and add additional data to resolve the discrepancies in the permeability data reported so far.

In this work we studied the H^+/OH^--permeability of DMPA bilayers by applying the stopped-flow method to produce a rapid pH change. A pH-sensitive absorbance indicator was

entrapped in the single lamellar vesicles. From the time course of the absorbance change after the pH jump and the known vesicle size the permeability could be calculated.

Materials and Methods

Dinyristoyl phosphatidic acid (DMPA) of 99% purity as tested by TLC was purchased from FLUKA (Neu-Ulm, F.R.G.) and used without further purification. Sephadex G-100 and G-25 were products of Pharmacia (Uppsala, Sweden). Analytical grade Cresol red (*o*-cresolsulfonphthalein) was purchased from Merck (Darmstadt, F.R.G.). Unilamellar DMPA vesicles can be prepared without prolonged sonication or the necessity to apply the injection method. The following procedure gives suspensions with reproducible vesicle diameters: a weighed amount of the disodium salt of DMPA was suspended in a 0.01 M Cresol red solution in 0.01 M NaOH. The suspension was vortexed and then sonicated for 1 min using a MSE Ultrasonic Disintegrator with a 1/2 inch titanium tip. After adjusting the pH with dilute HCl to pH 7.5 the vesicle suspension was annealed at 60°C for 1 h *. Extra-vesicular cresol red was removed by filtration through a Sephadex G-100 (3 × 35 cm) column. Possible multilamellar structures were removed by filtration through a 0.45 μm Millipore filter. The phospholipid concentration in the final vesicle suspension was determined by phosphorus analysis using a modified procedure of Hague and Bright [21]. The DMPA vesicles were characterized by freeze-fracture electron microscopy. The vesicles are single-walled with diameters between 50 and 240 nm.

The time course of Cresol red leakage was measured by incubating the vesicle suspension either below or above the DMPA phase transition for a certain time, filtering the vesicle suspension through a Sephadex G-25 column and then measuring the absorbance at 572 nm using a Perkin-Elmer Model 124 spectrophotometer.

For the kinetic measurements a Durrum Model D 110 Stopped-flow spectrophotometer was used. The instrumental dead time was determined to 1–2 ms. The temperature of the reactants was kept constant to ±0.5 K using a MGW Lauda thermostat. The time course of the absorbance change at 572 nm after rapid mixing was followed using a Datalab DL 905 transient recorder. Absorbance vs. time curves were stored in a home-built 64k solid state memory [22] and subsequently read into a Hewlett-Packard 9845A computer for further data processing.

Results

Fig. 1 shows absorbance spectra of an aqueous solution of Cresol red at different pH values. The intensities of the 420 nm and the 572 nm band depend on the following equilibrium:

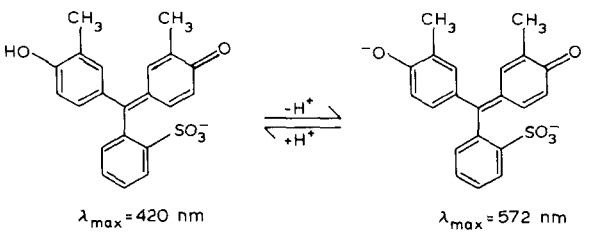

In water a pK of 7.75 was found for the equilibrium between the singly and doubly charged form of the indicator. As Cresol red is negatively charged in both forms it can be easily entrapped in vesicles of a negatively charged phospholipid such as phosphatidic acid. Thus it can serve as an indicator for the intra-vesicular pH. In the stopped-flow experiment the DMPA-vesicle suspension (pH 7.5) is rapidly mixed with an equal

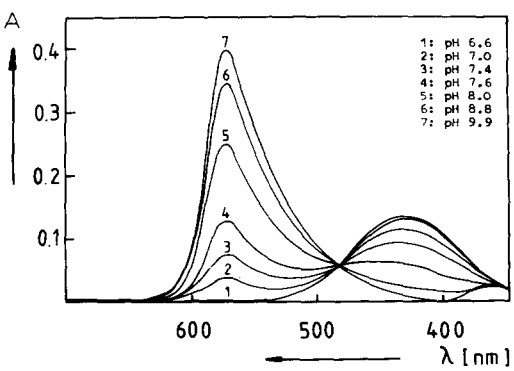

Fig. 1. Absorption spectra of an aqueous Cresol red solution at various pH values ($c = 5.2 \cdot 10^{-6}$ M, 25°C).

* During the preparation of this manuscript we became aware of paper by Hauser and Gains [32] in which a similar method for preparing phosphatidic acid vesicles is described.

volume of dilute HCl or NaOH, respectively. The time course of the absorbance of the entrapped indicator can then be followed. The absorbance should change according to the following expression:

$$A(t) = A(\infty) - \{A(\infty) - A(0)\} \exp[-k_D \cdot t] \quad (1)$$

where $A(t)$, $A(0)$ and $A(\infty)$ are the absorbance at time t, before the pH jump and at the end of the reaction, respectively. As the indicator equilibrium itself is reached very fast the time constant k_D should be related to the rate limiting step, i.e. the permeation of protons and hydroxyl ions through the bilayer membrane. From the rate constant k_D the permeability coefficient P can be calculated. As the bilayer thickness is small compared to the vesicle diameter it can be neglected and we can use the following equation:

$$k_D = P \cdot F/V = 3P/r \quad (2)$$

where F is the surface area, V the volume and r the radius of the vesicles. It should be mentioned that it is not possible to discriminate between proton and hydroxyl ion permeation, only an average permeability coefficient P_{net} can be determined. A prerequisite for the calculation of P_{net} however is the knowledge of the vesicle radius r. A histogram of the size distribution of the DMPA vesicles as determined from freeze-fracture electron micrographs is shown in Fig. 2. The major fraction consists of vesicles with a radius between 50 and 90 nm. Two other small fractions with 25–35 nm and 120–130 nm radius are also present. Thus we cannot expect to observe only a single time constant but several different ones which have to be consistent with the vesicle size distribution. In addition we have to prove that the indicator is not leaking from the vesicles. We tested for indicator leakage by incubating the vesicle suspension above or below the DMPA phase transition temperature and then determining the residual entrapped Cresol red concentration as described in Materials and Methods. Fig. 3 shows the time course of Cresol red leakage at two different temperatures. Below the transition temperature T_m there is almost no leakage inside a period of 4 h, whereas at 65°C permeation has a half-time of approx. 50 min. In any case, indicator leakage is very slow compared

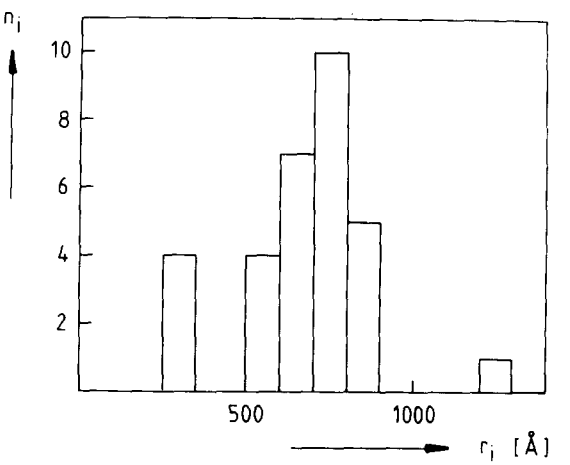

Fig. 2. Size distribution of Cresol red-containing DMPA vesicles determined by freeze-fracture electron microscopy. The vesicles were prepared as described in Materials and Methods. n_i is the number of vesicles with radius r_i.

to the observed absorbance changes due to H^+/OH^- permeation, so that this effect can be neglected. In an additional test we attempted to determine the localization of the indicator molecule. As the indicator is negatively charged between pH 5 and pH 10 it seemed unlikely that the probe molecule would dissolve into the hydrophobic part of the bilayer or bind to the negatively charged surface of the vesicles. In fact the distribu-

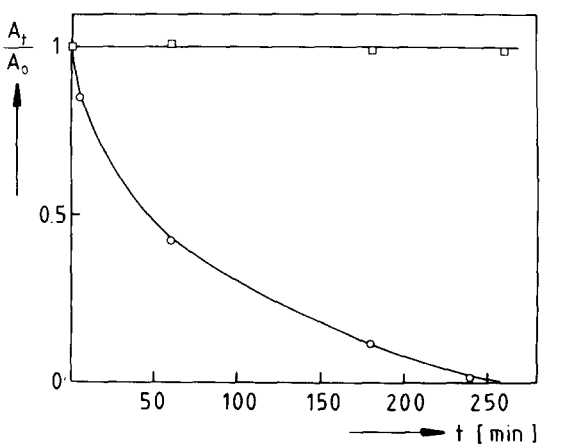

Fig. 3. Time course of Cresol red efflux from DMPA vesicles on incubation at 25°C (□) and 65°C (○). A_0 and A_t, the absorbance of the lipid fraction immmediately after preparation and at time t, respectively. Absorbance was measured at 572 nm.

tion coefficient of Cresol red between *n*-hexane and water is so small that no indicator could be spectrophotometrically detected in the organic phase when an aqueous solution of Cresol red was extracted with *n*-hexane. Titration experiments of cresol red entrapped in DMPA vesicles showed a shift of the apparent pK to higher values (see Fig. 4). However, the absorption spectrum of Cresol red in these vesicle suspensions remains unchanged and is not influenced by the phase transition. So the chromophore of the indicator is definitely not located in the hydrophobic part of the bilayer. The shift of the pK and the asymmetry of the titration curve can be explained by the fact that we are dealing with vesicles with a negatively charged surface. This leads to a local increase in the proton concentration close to the surface [23] and thus to a non-uniform distribution of the Cresol red anions in the vesicle interior. The higher proton concentration shifts the equilibrium

$$H_2O + (\text{Cresol red})^- \rightleftharpoons (\text{Cresol Red})^{2-} + H_3O^+ \qquad (3)$$

to the left thus increasing the apparent pK. However this has no effect on the experimental results as we always measure absorbance changes.

Fig. 5 shows the change of the absorbance spectrum and the time course of the intensity increase of the 572 nm band after mixing equal volumes of

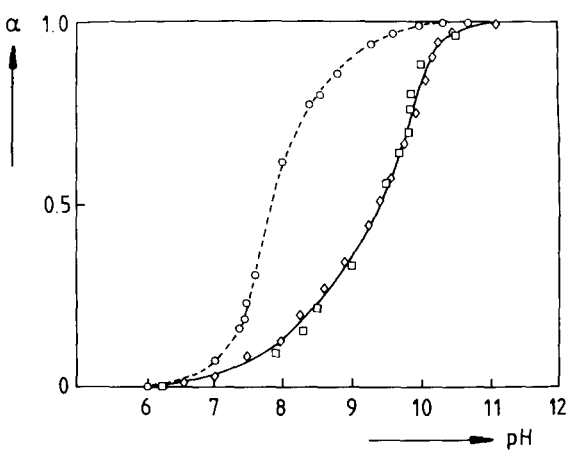

Fig. 4. Titration curves of Cresol red in water and in DMPA vesicles. - - - - - -, aqueous solution, 25°C; pK = 7.75. ———, Cresol red entrapped in DMPA vesicles; pK = 9.35. ◇, at 25°C; □, at 58°C. The degree of dissociation α was calculated from the intensity of the 572 nm band (see Fig. 1).

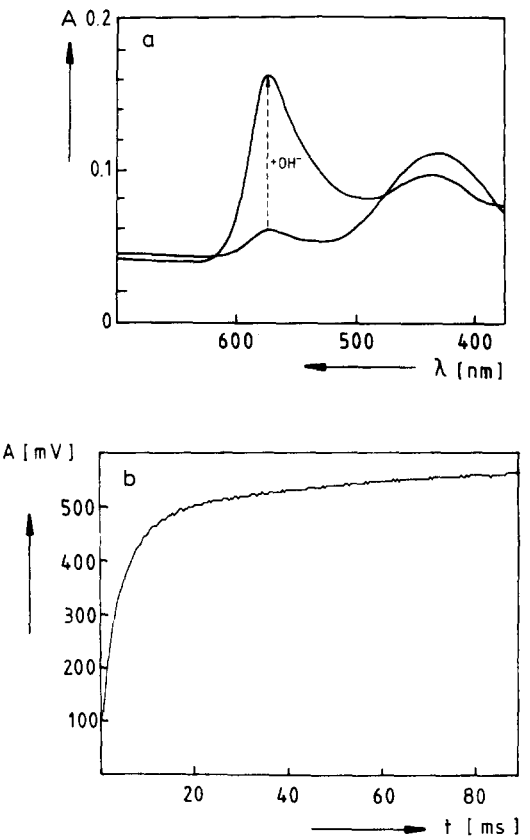

Fig. 5. (a) Change of the absorbance spectrum of a DMPA vesicle solution after mixing with an equal volume of 1 mM NaOH solution. (b) Time course of the absorbance at 572 nm (photomoltiplier voltage; 10 mV ≡ 0.001 A) After mixing of Cresol red-containing DMPA vesicles (c = 0.21 mM, pH 7.5) with a 1 mM NaOH solution. T = 25°C, pH jump from 7.5 to 9.2.

a DMPA-vesicle suspension and a 1 mM NaOH solution thus producing a pH jump from 7.5 to 9.2. Clearly two processes with different time constants are observed. The time range for the half-times $t_{1/2}$ for the two processes and their relative amplitudes are summarized in Table I. The existence of two processes with different time constants can be explained on the basis of the vesicle size distribution (see Fig. 2). The slower reaction can be attributed to H^+/OH^- permeation into the large vesicles with 120 nm radius. Though this fraction comprises only approx. 4% of the main fraction, these vesicles contain approx. 20% of the indicator molecules as their internal volume is much larger. In agreement with this we find an

TABLE I

KINETICS OF PROTON/HYDROXYL ION PERMEATION ACROSS DMPA BILAYERS

pH jump from 7.5 to 9.2. Half-times $t_{1/2}$ and relative amplitudes ΔA for the fast(1) and slow(2) kinetic phases (see text). T_m = transition temperature at pH 7.5 (53°C).

Temperature	$t_{1/2}$ (1) (ms)	ΔA(1)	$t_{1/2}$(2) (ms)	ΔA(2)
$T < T_m$	50–200	70%	200–1200	30%
$T > T_m$	3–6	80%	20–40	20%

amplitude change of roughly 20 to 30% for the slow reaction. While the larger amplitude change is connected with the main vesicle fraction the third process expected from the vesicle size distribution can obviously not be observed. This reaction is clearly faster than the instrumental dead time. In fact the total amplitude change observed in the stopped-flow experiment is always smaller than expected from the steady-state measurements (see Fig. 5a), a clear indication that indeed an additional fast reaction is present which can not be resolved by the stopped-flow method.

Fig. 6 shows the temperature dependence of the half-times for H^+/OH^--permeation when we use an pH jump from 7.5 to 9.2. The permeability increases drastically above the transition temperature of DMPA when the bilayers are in the liquid-crystalline state. In a completely analogous experiment we mixed the DMPA vesicle suspension with 1 mM HCl. This produces a pH jump from 7.5 to 3.5. The absorbance change at 572 nm was monitored as before. The absorbance decreases as expected from the steady-state measurements (see Fig. 1). Again two different processes were observed with approximately the same relative amplitudes as in the previous experiment. Though both processes are slightly faster than in the experiment using a pH jump from 7.5 to 9.2 the temperature dependence of the half-times is very similar (see Fig. 7). An Arrhenius plot of the rate constant $k_1 = \ln(2/t_{1/2}(1))$ for the faster process is shown in Fig. 8. From the slope of the curves in the temperature range above T_m the activation energy for H^+/OH^- permeation through liquid-crystalline DMPA bilayers can be calculated to be approx. 20 kcal/mol. Though there are measurable differences in the rate constant when both experiments are compared the activation energies are approximately the same. We do not have sufficient experimental data for an accurate determination of the activation energy in the gel state. However, as can be seen from Fig. 8 the slopes of the curves in the gel state region seem to be very similar so that no large differences are to be expected.

Permeability constants calculated from the rate constant k_1 of the fast process using a mean

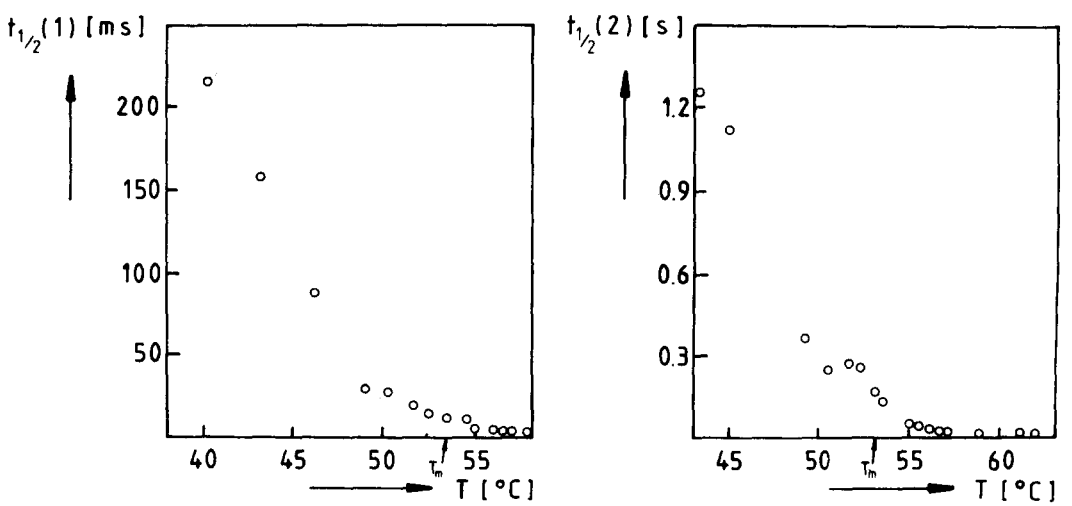

Fig. 6. Temperature dependence of the half-times $t_{1/2}$ (1) and $t_{1/2}$ (2). pH jump from 7.5 to 9.2. See text for further explanations.

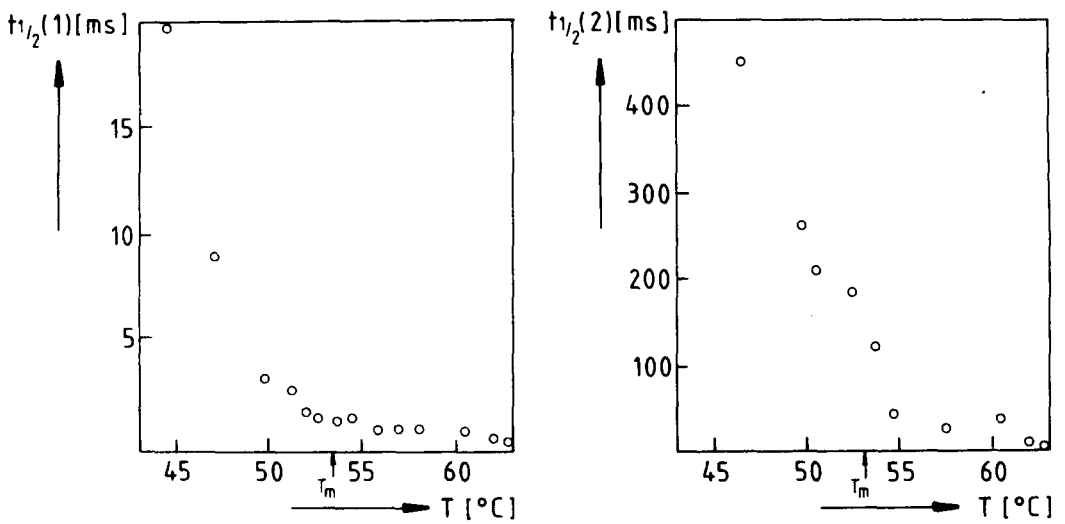

Fig. 7. Temperature dependence of the half-times $t_{1/2}$ (1) and $t_{1/2}$ (2) for a pH jump from 7.5 to 3.5. See text for further explanations.

vesicle radius of 70 nm are listed in Table II. The values for P_{net} are high and are in the range between $1 \cdot 10^{-5}$ and $1 \cdot 10^{-3}$ cm · s^{-1}. Slightly lower values are calculated from the rate constants for the slower process. These however are not as accurate, as the amplitude for this reaction is small complicating the precise determination of rate constants.

In addition to the fast processes observed in the stopped-flow experiments a much slower reaction with half-times between 5 and 0.3 min is present. This reaction can be easily followed using a conventional spectrophotometer. The absorbance change for this reaction is very small, typically only 10% of the total absorbance change. The half times for this reaction as a function of temperature are listed in Table III. The temperature dependence for this reaction is completely different as a minimum in the half-time is observed at the phase transition temperature (53°C) corresponding to a maximum of the permeability coefficient. At 45°C the permeability coefficient is calculated to $1 \cdot 10^{-8}$

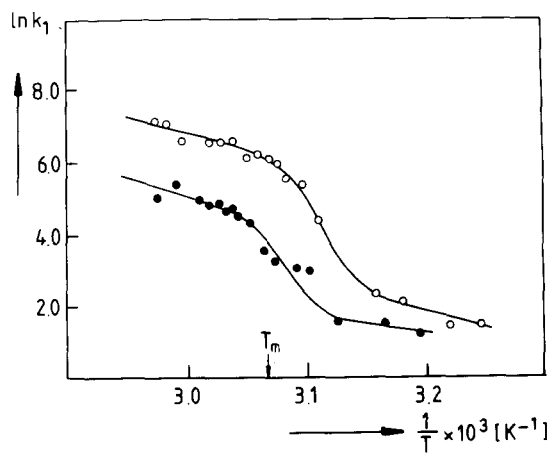

Fig. 8. Arrhenius plot of the rate constant k_1 for H^+/OH^- diffusion through DMPA bilayers: (○) pH jump from 7.5 to 3.5; (●) pH jump from 7.5 to 9.2.

TABLE II

RATE CONSTANTS AND CALCULATED PERMEABILITY COEFFICIENTS FOR H^+/OH^- DIFFUSION ACROSS DMPA BILAYERS

Temp. (°C)	Acidified		Alkalinized	
	k_1 [a] (s^{-1})	P_{net} [b] (cm·s^{-1}) ($\times 10^6$)	k_1 [a] (s^{-1})	P_{net} [b] (cm·s^{-1}) ($\times 10^6$)
35.0	4	9	3	7.0
53.2 [c]	518	1200	55	130
65.0	1408	3300	200	470

[a] Data from Fig. 8.
[b] Calculated according to Eqn. 2 with $r = 70$ nm.
[c] DMPA transition temperature at pH 7.5.

TABLE III

TEMPERATURE DEPENDENCE OF THE HALF-TIME $t_{1/2}(3)$, THE COUNTERION CONTROLLED KINETIC PHASE

pH jump from 7.5 to 3.5.

Temperature (°C)	$t_{1/2}(3)$ (min)
45.0	2.5
49.6	1.0
52.5	0.5
54.2	0.5
56.0	0.7
57.8	0.7
59.6	0.7
64.0	0.6

$cm \cdot s^{-1}$. Extrapolation to 25°C leads to a value of approx. $1.5 \cdot 10^{-10}$ $cm \cdot s^{-1}$. Thus the permeability calculated from the slow kinetic phase is by several orders of magnitude lower.

Discussion

Our results support the suggestion made by Nichols and Deamer [5] and Clement and Gould [7] that H^+/OH^- diffusion proceeds essentially in two consecutive steps. In the case of a pH jump to 3.5 when a large proton gradient is applied the initial fast permeation of the protons through the bilayer membrane leads to an accumulation of positive charges in the vesicle interior and therefore to the formation of a transmembrane potential. This fast permeation is only possible as long as the free energy difference caused by the pH-gradient overcompensates the energy required for charge separation. After this initial fast kinetic phase proton transport is coupled to counterion diffusion which is much slower. The counterion can be Cl^- in case of a HCl induced pH jump but charge compensation could also be effected by diffusion of sodium ions from the vesicle interior. In agreement with these suggestions Biegel and Gould [8] found that the slow phase can be accelerated when valinomycin as a carrier for alkali cations is added to the vesicle suspension. Gramicidin on the other hand, a pore former, enhances both the slow and the fast kinetic process, because protons as well as other cations can diffuse through the gramicidin pores. In our case evidence that the slow kinetic phase is connected with counterion diffusion comes from the characteristic temperature dependence of this process. We found the for ion permeation characteristic maximum for the permeability coefficient at the phase transition temperature [13,17,18,24]. Water permeation on the other hand is characterized by a jump of the permeability at the phase transition [18,19]. As mentioned above there are large discrepancies reported in the literature for the permeation of protons and hydroxyl ions. Table IV summarizes some of the experimental data. Values for non-electrolyte permeation are also included. There is no simple explanation for the differences between data incicating high and very low H^+/OH^- permeability. It has been suggested that diffusion of molecular HCl contributes to the high proton permeability of membranes when a large proton gradient is induced using hydrochloric acid [10]. This effect can be excluded in our case as we find within experimental error the same high permeability when we use H_2SO_4 instead of HCl or jump into the alkaline pH-region using NaOH. As can be seen from Table IV our experimental results are similar to those reported by Nichols and Deamer [5], Nichols et al. [6], Biegel and Gould [8], and Rossignol et al. [12]. In agreement with these workers we propose a H^+/OH^- permeation mechanism which is different from other ions. A comparison of the data in Table IV supports the assumption that H^+/OH^-- and H_2O-permeation are interrelated. Additional support comes from the experimental finding that the temperature dependence of the permeability is similar to that of H_2O diffusion [19] and does not display the for ions characteristic maximum at the phase transition temperature. Only a sudden increase of the permeability in the liquid-crystalline phase is observed.

The permeability coefficients measured using a pH jump from 7.5 to 3.5 are about one order of magnitude higher than those determined using a pH jump to 9.2. Two different effect may account for this phenomenon, namely a change in the surface charge density of the bilayer and a change in the individual contributions of protons and hydroxyl ions to the observed net permeability. Changes in the external pH lead to alteration in

TABLE IV

PERMEABILITY DATA FOR PERMEATION ACROSS LIPID BILAYERS

Abbreviations: PC, phosphatidylcholine; PS, phosphatidylserine; PA, phosphatidic acid; DPPC, dipalmitoylphosphatodylcholine; DMPA, dimyristoyl phosphatidic acid; RT, room temperature

Permeant	Lipid system	P ($cm \cdot s^{-1}$)	Temp.	Ref.
H^+/OH^-	DMPA vesicles	10^{-5}	35°C	this
	DMPA vesicles	$(1-10) \cdot 10^{-4}$	65°C	work
	PC/PA vesicles	10^{-4}	RT	6
	PS vesicles	$6.5 \cdot 10^{-4}$	RT	5
	Soy bean lipids	10^{-4}	25°C	8
	Horse bean lipids	10^{-4}	25°C	12
	PC/cholesterol [a]	$(3-4) \cdot 10^{-9}$	24°C	10
	Egg yolk PC vesicles	$< 10^{-12}$	RT	11
Na^+	Egg yolk PC vesicles	$\approx 10^{-12}$	RT	11
Cl^-	PS vesicles	$6.5 \cdot 10^{-12}$	RT	24
H_2O	DPPC vesicles	$3.5 \cdot 10^{-5}$	37°C	19
	DPPC vesicles	$2.4 \cdot 10^{-3}$	46°C	19
HCl	Egg yolk PC vesicles	$3 \cdot 10^{-3}$	RT	11

[a] Experiments using planar lipid membranes.

the degree of dissociation of the DMPA headgroup [25–27]. At pH 7.5 DMPA carries one negative charge. A jump to pH 9.2 increases the negative surface charge. Thus the hydroxyl ions, which give the main contribution to the observed net H^+/OH^- flux as their concentration is approximately four orders of magnitude higher, are repelled even more from the bilayer surface. A jump to pH 3.5 reduces the negative suface charge. However, in this case the proton is the main species contributing to the flux and there is no electrostatic repulsion as the surface is still negatively charged. Thus permeability is expected to be much higher. Due to this surface charge effect vesicles prepared from DMPA show large differences in the permeability depending on whether pH jump into the alkaline or the acidic pH region is employed. The differences observed for neutral lipids using different pH jumps are much smaller as the individual contributions of protons and hydroxyl ions to the net permeability are not changed to such a large degree [12]. In addition, changes in the surface charge density of DMPA vesicles lead to alterations in chain packing in the gel state [28]. This should have an influence on the permeability properties. However, we believe that this is of minor importance and that the observed differences can be explained by taking into account only the electrostatic effects at the bilayer surface.

The several orders of magnitude lower permeability values reported by Nozaki and Tanford [11] were possibly obtained under conditions where counter-ion diffusion was rate limiting [9]. As we could show, the use of large pH gradients across lipid bilayer membranes does produce diffusion potentials leading to biphasic diffusion kinetics. The apparent permeability coefficient we determined from the slow kinetic phase is in the range of 10^{-9} $cm \cdot s^{-1}$. Its temperature dependence reveals the characteristic maximum at the phase transition generally found for the permeation of larger ions.

Two different models for the permeation of small molecules through bilayer membranes have been proposed, the diffusion and the pore model. Whereas the first generally gives a good description for the permeation of non-electrolytes through lipid bilayers the calculated H_2O permeability is too low by at least one order of magnitude [29]. The second model on the other hand fails in predicting the high activation energy (approx. 20 kcal/mol) for water permeation [30,31]. In the

special case of H_2O- and H^+/HO^--permeation an alternative assumption is that water molecules present in the hydrophobic interior of the membrane are at least partly associated via hydrogen bonds. Protons and hydroxyl ions could use this preexisting network of associated water molecules for transport in an analogous mechanism as is found for the proton conductance in ice and water. This was first suggested by Nichols and Deamer [5]. The high activation energy found for H^+/OH^- permeation could then be explained by the necessity to break several hydrogen bonds when protons or hydroxyl ions are 'transported' through the bilayer [12]. The higher permeability above the phase transition temperature, on the other hand, results from an increase in the number of associated water molecules and should have no effect on the activation energy.

In summary we could show that H^+/OH^- permeation across DMPA bilayers is fast in the initial phase and slow when counterion diffusion is the rate limiting step. Both kinetic phases can be differentiated on the basis of their temperature dependence. The initial fast electrically uncompensated H^+/OH^- permeation shows no maximum at the phase transition temperature but only a jump. It has a high activation energy and thus is similar to water permeation. The slow kinetic phase dislays the typical maximum of the permeability at the transition temperature, which is generally found for the diffusion of ions through lipid bilayers. The high H^+/OH^- permeability supports the hypothesis that proton and hydroxyl ion diffusion proceeds via associated water molecules.

Acknowledgements

We gratefully acknowledge the help of Dr. W. Welte, Institut fuer Biophysik und Strahlenbiologie, for providing us with the freeze-fracture electron micrographs. We also thank Professor Dr. T. Ackermann for his continuous support and advice. This work was supported by the Deutsche Forschungsgemeinschaft.

References

1 Mitchell, P. and Moyle, J. (1967) Biochem. J. 104, 588–600
2 Henning, R. (1975) Biochim. Biophys. Acta 401, 307–316
3 Toll, L. and Howard, B. (1978) Biochemistry 17, 2517–2523
4 Rottenberg, H. (1979) Methods Enzymol. 55F, 547–569
5 Nichols, J.W. and Deamer, D.W. (1980) Proc. Natl. Acad. Sci. U.S.A. 77, 2038–2042
6 Nichols, J.W., Hill, M.W., Bangham, A.C. and Deamer, D.W. (1980) Biochim. Biophys. Acta 596, 393–403
7 Clement, N.R. and Gould, J.M. (1981) Biochemistry 20, 1534–1538
8 Biegel, C.M. and Gould, J.M. (1981) Biochemistry 20, 3474–3479
9 Deamer, D.W. and Nichols, J.W. (1982) Biophys. J. 37, 121a
10 Gutknecht, J. and Walter, A. (1981) Biochim. Biophys. Acta 641, 183–188
11 Nozaki, Y. and Tanford, C. (1981) Proc. Natl. Acad. Sci. U.S.A. 78, 4324–4328
12 Rossignol, M., Thomas, P. and Grignon, C. (1982) Biochim. Biophys. Acta 684, 195–199
13 Papahadjopoulos, D., Jacobson, K., Nir, S. and Isac, T. (1973) Biochim. Biophys. Acta 311, 330–348
14 Wu, S. and McConnell, H.M. (1973) Biochem. Biophys. Res. Commun. 55, 484–491
15 Tsong, T.Y. (1975) Biochemistry 14, 5409–5414
16 Marsh, D., Watts, A. and Knowles, P.F. (1976) Biochemistry 15, 3570–3578
17 Block, M.C., Van der Neut-Kok, E.C.M., Van Deenen, L.L.M. and De Gier, J. (1975) Biochim. Biophys. Acta 406, 187–196
18 Kanehisa, I.M. and Tsong, T.Y. (1978) J. Am. Chem. Soc. 100, 424–432
19 Lawaczeck, R. (1979) J. Membrane Biol. 51, 229–261
20 Elamrani, K. and Blume, A. (1982) Biochemistry 21, 521–526
21 Hague, J.L. and Bright, H.A. (1940) J. Res. Natl. Bur. Stand. 26, 405–407
22 Messner, G. (1978) Diploma thesis, University of Freiburg
23 Vaz, W.L.C., Nicksch, A. and Jähnig, F. (1978) Eur. J. Biochem. 83, 299–305
24 Papahadjopoulos, D., Nir, S. and Ohki, S. (1972) Biochim. Biophys. Acta 266, 561–583
25 Träuble, H. and Eibl, H. (1974) Proc. Natl. Acad. Sci. U.S.A. 71, 214–219
26 Eibl, H. and Blume, A. (1979) Biochim. Biophys. Acta 553, 476–488
27 Blume, A. and Eibl, H. (1979) Biochim. Biophys. Acta 558, 13–21
28 Jähnig, F., Harlos, K., Vogel, H. and Eibl, H. (1979) Biochemistry 18, 1495–1468
29 Stein, W.D. (1967) in The Movement of Molecules Across Cell Membranes, pp. 65–125, Academic Press, London, New York
30 Price, H.D. and Thompson T.E. (1969) J. Mol. Biol. 41, 443–457
31 Andrasko, J. and Forsen, S. (1974) Biochem. Biophys. Res. Commun. 60, 813–819
32 Hauser, H. and Gains, N. (1982) Proc. Natl. Acad. Sci. U.S.A. 79, 1638–1687